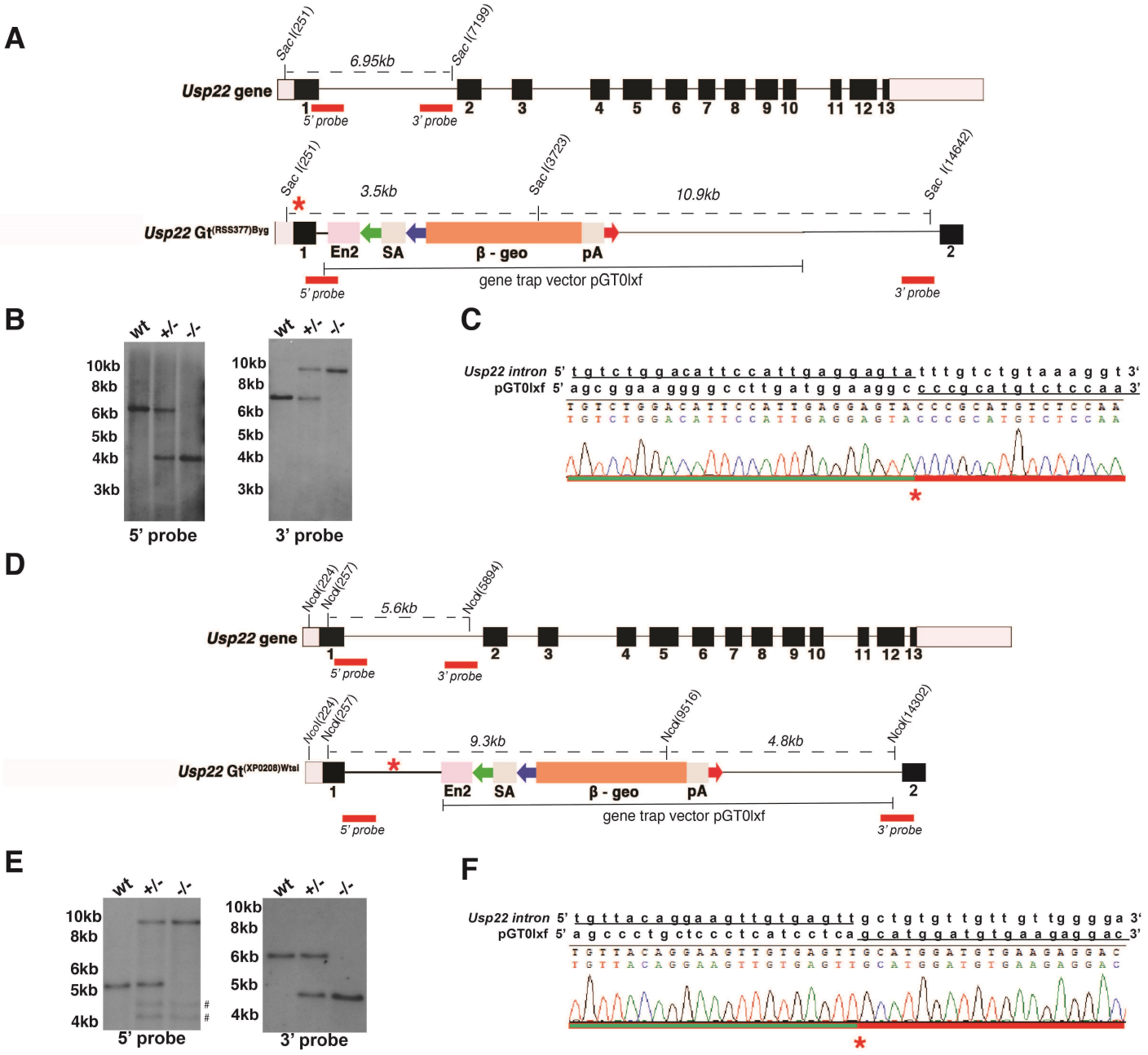

Fig. S1. Characterization of targeted integrations in the Usp22 locus in mouse embryonic stem cells generated by the International Gene Trap Consortium (IGTC). (A, D) Graphs of the gene trap vector integration in Usp22 locus in the two different mouse embryonic stem cell lines generated by the IGTC. (B, E) Southern blot analysis of the targeted loci with the probes shown in the graphs for the two different mouse embryonic stem cell lines. (C, F) Sanger sequencing analysis of the exact integration point of the gene trap vector pGT0lxf in the Usp22 locus in the two different mouse embryonic stem cell lines.

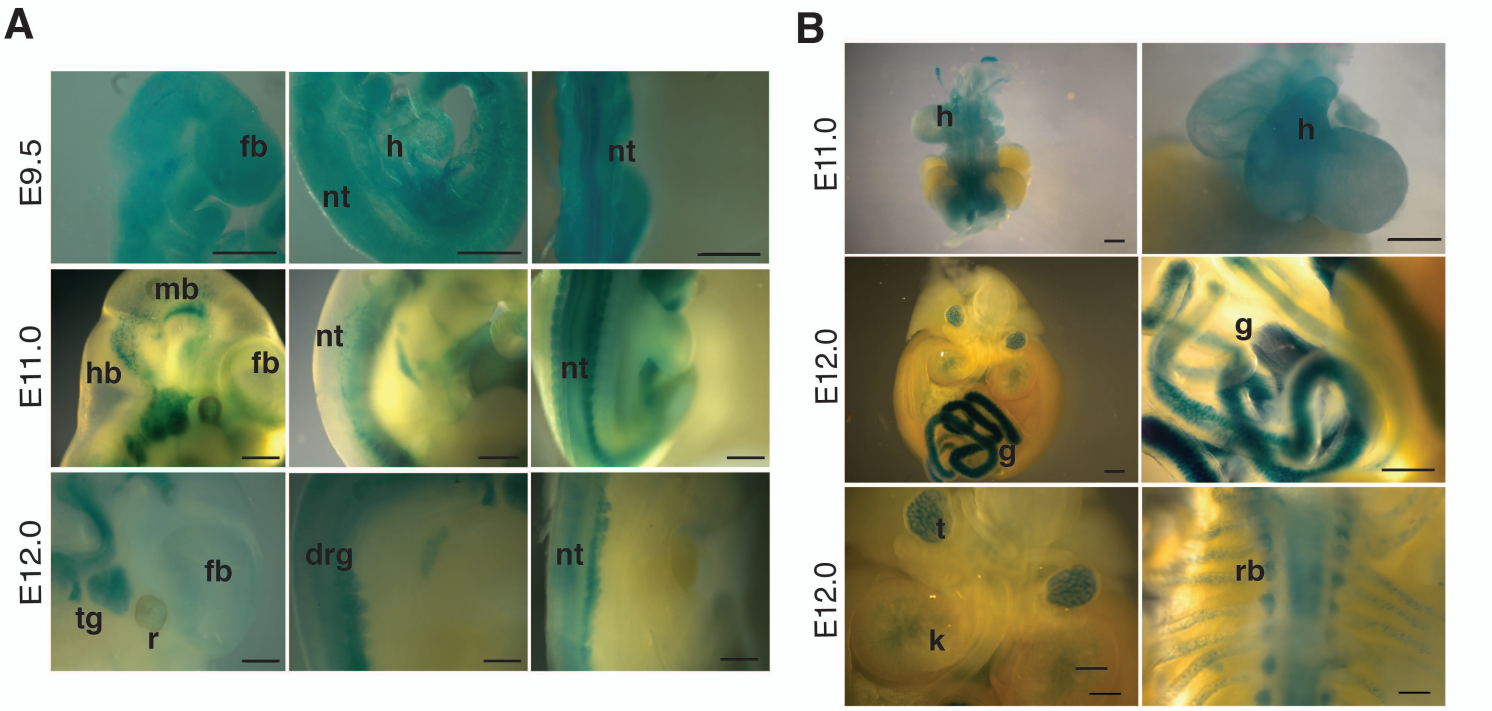

Fig. S2. Usp22 expression pattern in the developing embryo. (A, B) LacZ stainings of Usp22-Gt (RRS377) Byg heterozygous embryos show Usp22 expression in the developing neuroectoderm as well as in organs of mesodermal origin. fb forebrain, mb midbrain, hb hindbrain, h heart, nt neural tube, tg trigeminal ganglion, r retina, drg dorsal root ganglia, g gut, k kidney, t testis, rb ribs. Scale bar 200um

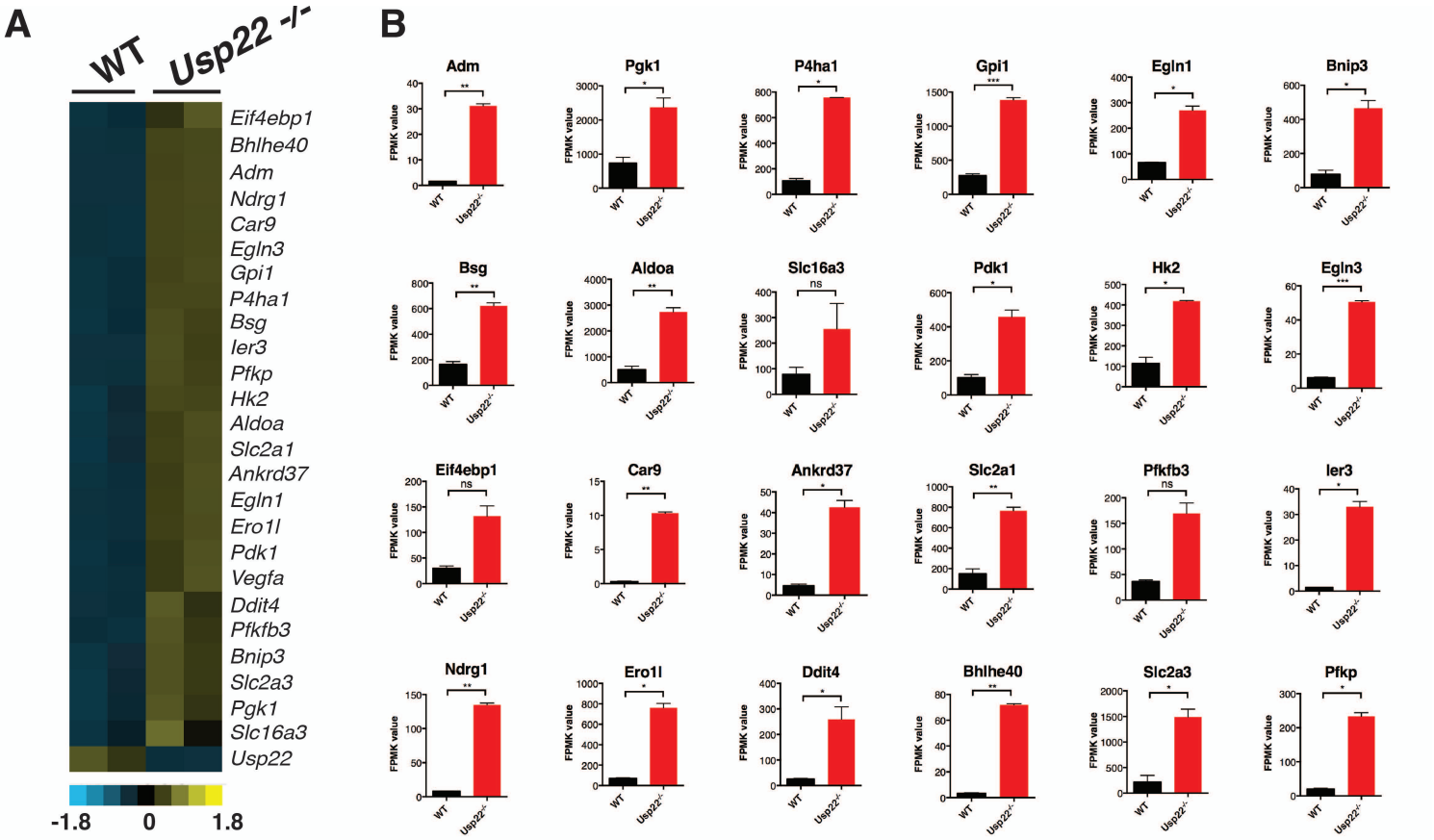

Fig. S3. Differential expression of genes involved in hypoxic stress response in *Usp22* $^{-/-}$ embryos. (A) Heat map of differentially expressed genes induced by hypoxic response in wild-type and *Usp22* mutant embryos at E10.5. (B) RNA-seq data of wild type and *Usp22* mutant embryos at E10.5 showing expression of genes induced by hypoxia. Bar graphs show FPKM (fragments per kilobase of exon per million reads mapped) values. Error bars represent SD of wild-type (n=2) and *Usp22* $^{-/-}$ (n=2). *p-value (p<=0.05) calculated by unpaired t-test with Welch's correction.

A

Usp22-Gt$^{(RSS377)Byg}$	Genotype			Total number of pups analyzed
	+/+	+/-	-/-	
Observed number	234	453	0	687
Expected number	172	343	172	
Chi square	22.3	35.2	172	
p value	0.00001438	0.00000002	0.00000000	

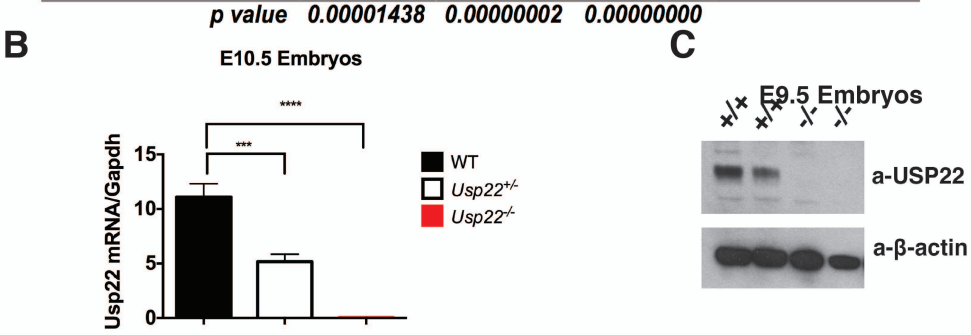

D

Usp22-Gt$^{(XP0208)Wtsi}$	Genotype			Total number of pups analyzed
	+/+	+/hyp	hyp/hyp	
Observed number	77	116	15	208
Expected number	52	104	52	
Chi square	12.09	1.38	26.32	
p value	0.0023	0.5	0.0000019	

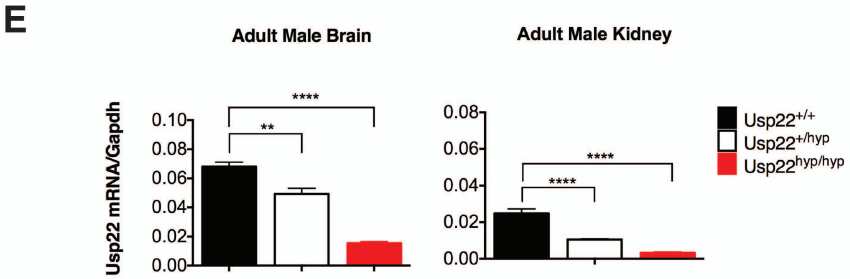

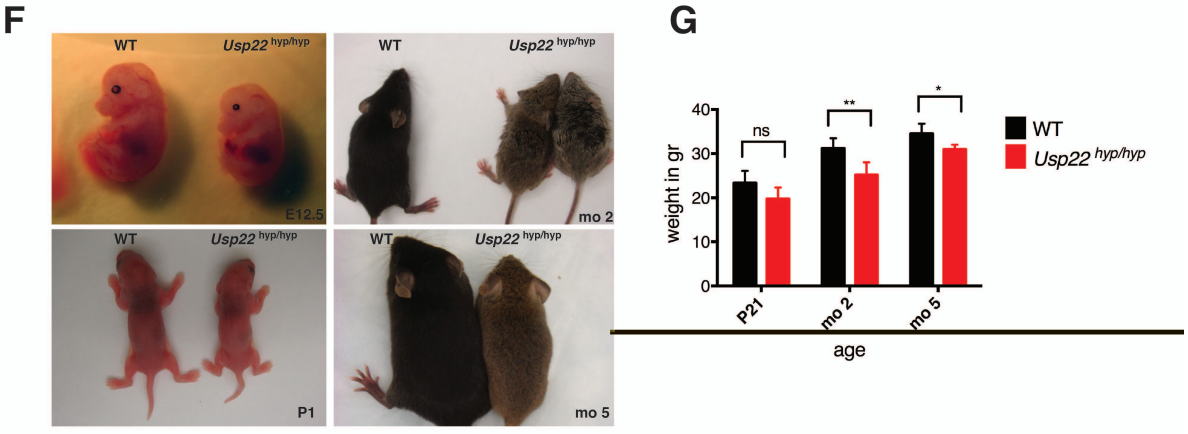

Fig. S4. Analysis of the Usp22 mouse lines generated by the implantation of the embryonic stem cells from the International Gene Trap Consortium. (A, D) Mendelian ratios of the respective number of adult mice collected from the two different mouse lines generated show Usp22-Gt (RRS377) Byg is a null allele, whereas Usp22-Gt (XP0208) Wtsi is a hypomorphic allele. (B, E) Quantitative expression analysis of Usp22 transcript in the null and the hypomorphic mouse lines generated. Error bars represent SD of three biological replicates. (C) Westerm blot analysis of total proteins collected from whole embryos at E9.5 that are either wild-type or null for Usp22 (Usp22 antibody generated by COVANCE and characterized in our lab). (F) Representative images of Usp22-Gt (XP0208) Wtsi animals at different ages show growth retardation of Usp22 hyp/hyp mice. (G) The body weight of male Usp22-Gt (XP0208) Wtsi miceis reduced on average by 15% compared to their littermates. Error bars represent SD of wild-type mice (n = 6) and Usp22 hyp/hyp mice (n = 6) that have been weighed at the indicated time points. *p-value (p<=0.05) calculated by unpaired t-test with Welch's correction.

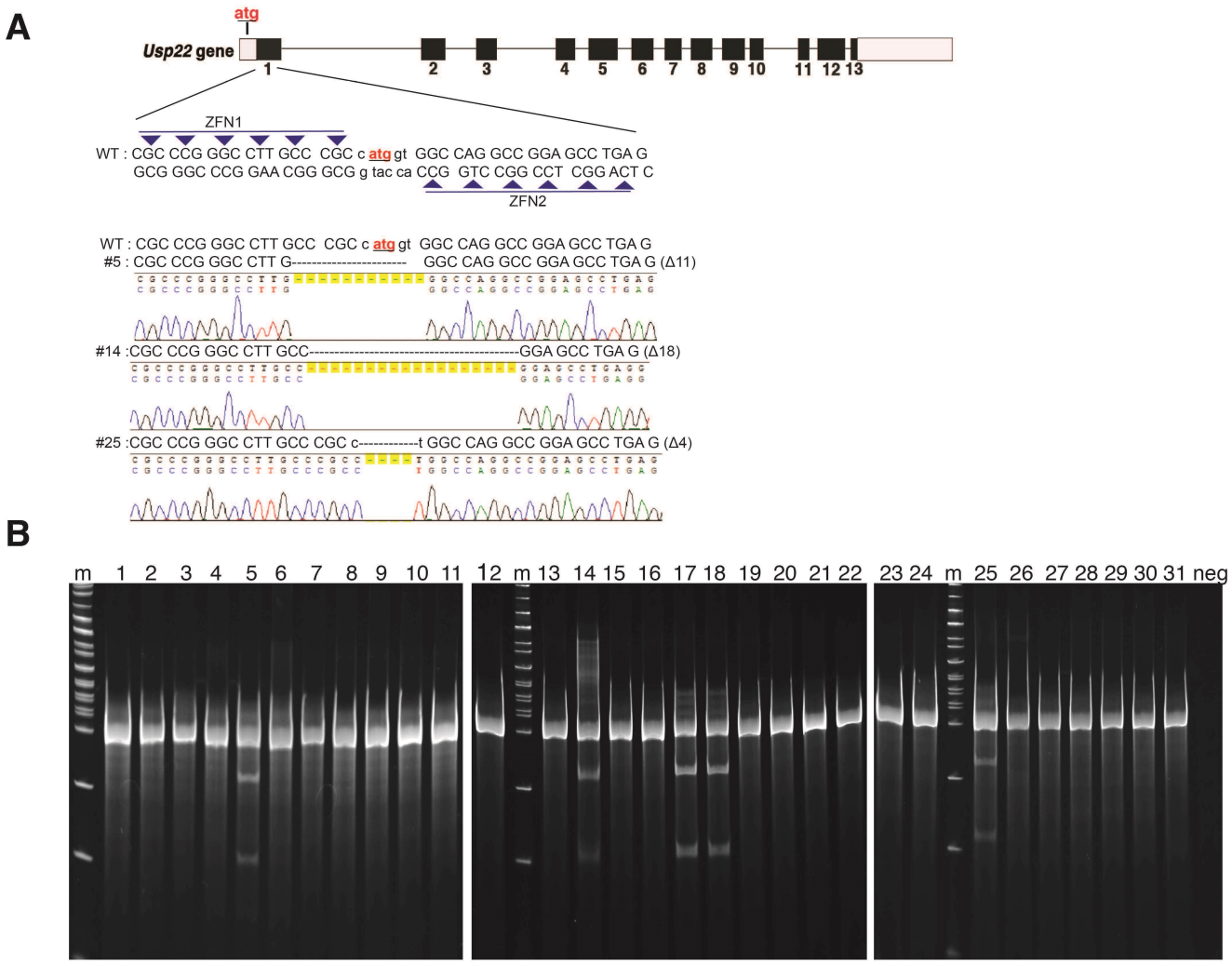

Fig. S5. Targeted deletion of Usp22 in mice using Zinc-Finger Nuclease (ZFN) technology. (A) Graph of the ZFN targeting sequence in the Usp22 locus and Sanger sequencing analysis of the 3 out of 5 founders produced after pronuclear injection of the ZFN mRNA in animals of FVB genetic background. (B) Representative Cel I assays performed on tail genomic DNA from 31 out of 43 pups born and products analyzed on 10% TBE SAGE gels.

A

Usp22^{14Zfn}	Genotype			Total number of pups analyzed
	+/+	+/-	-/-	
Observed number	38	61	0	*99*
Expected number	25	50	25	
Chi square	6.76	2.42	25	
p value	*0.034*	*0.29*	*0.000004*	

C

Usp22^{25Zfn}	Genotype			Total number of pups analyzed
	+/+	+/-	-/-	
Observed number	49	93	0	*142*
Expected number	35	72	35	
Chi square	5.6	6.2	35	
p value	*0.06*	*0.045*	*0.00000003*	

B

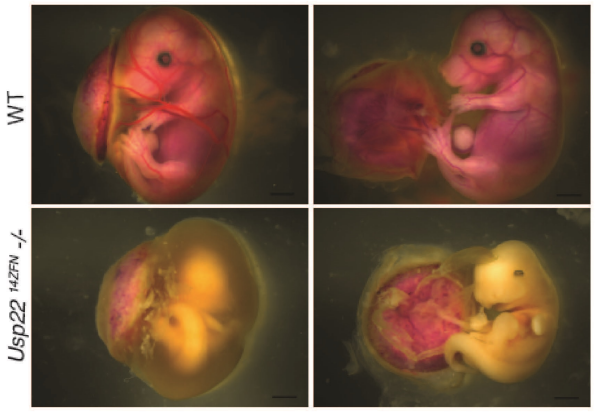

D

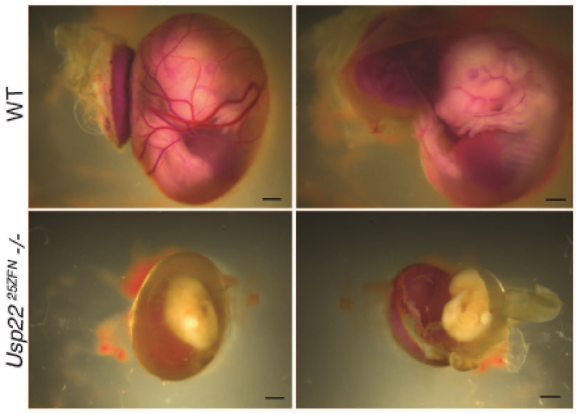

Fig. S6. Analysis of the embryonic lethality observed in embryos homozygotes for *Usp22* deletion. (A, C) Mendelian ratios of the respective number of adult mice collected from the two different mouse lines generated using zinc-finger nuclease technology show both *Usp22^{14zfn}* and *Usp22^{25zfn}* are null alleles. (B, D) Representative images of wild-type and homozygote embryos for Usp22 deletion at E16.5 that show similar embryonic lethal phenotype observed in the Usp22-Gt(RRS377) Byg homozygous embryos. Scale bar 2mm

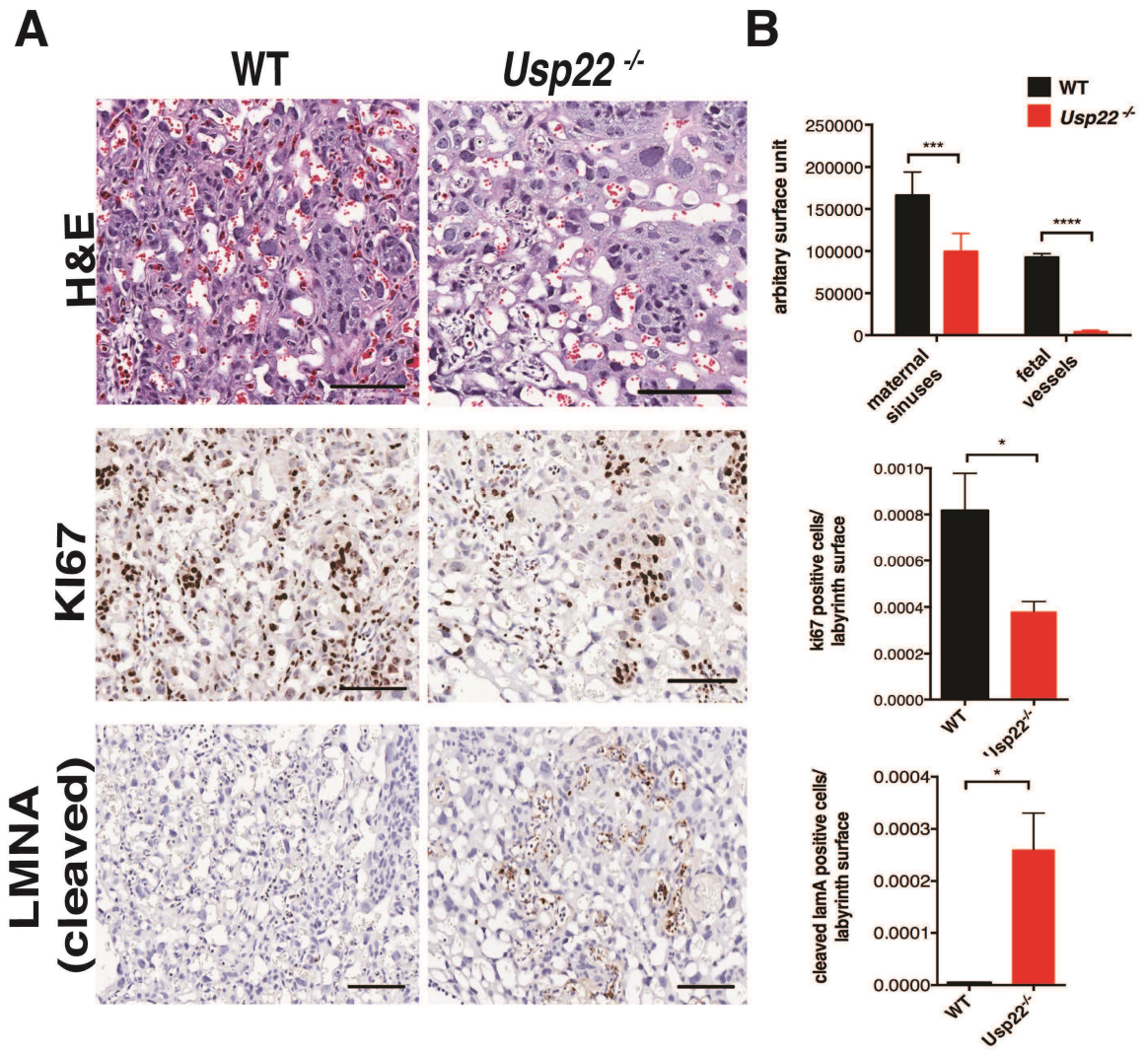

Fig. S7. Reduction in dividing labyrinth trophoblasts and increased apoptosis in fetal vessels is only observed in late developmental stages in Usp22 mutant placentas. (A) Placenta coronal sections from wild type and mutant Usp22 embryos at E12.5 stained with haematoxylin and eosin (H&E), KI67 and cleaved LAMIN A. Scale bar 100um (B) Quantification of maternal and fetal vessels using computational morphometry indicated that the number of fetal vessels in the labyrinth of Usp22 null embryos was much reduced compared with wild type littermates. Error bars represent SD of wild type sections (n=24), Usp22$^{-/-}$ sections (n=24). Quantification of proliferating and apoptotic cells on the same surface of wild-type and Usp22 mutant labyrinths show reduced proliferation and increased apoptosis at these later developmental stages. Error bars represent SD of at least n=100 positively stained cells in three placentas per genotype. *p<=0.05 calculated by unpaired t-test with Welch's correction.

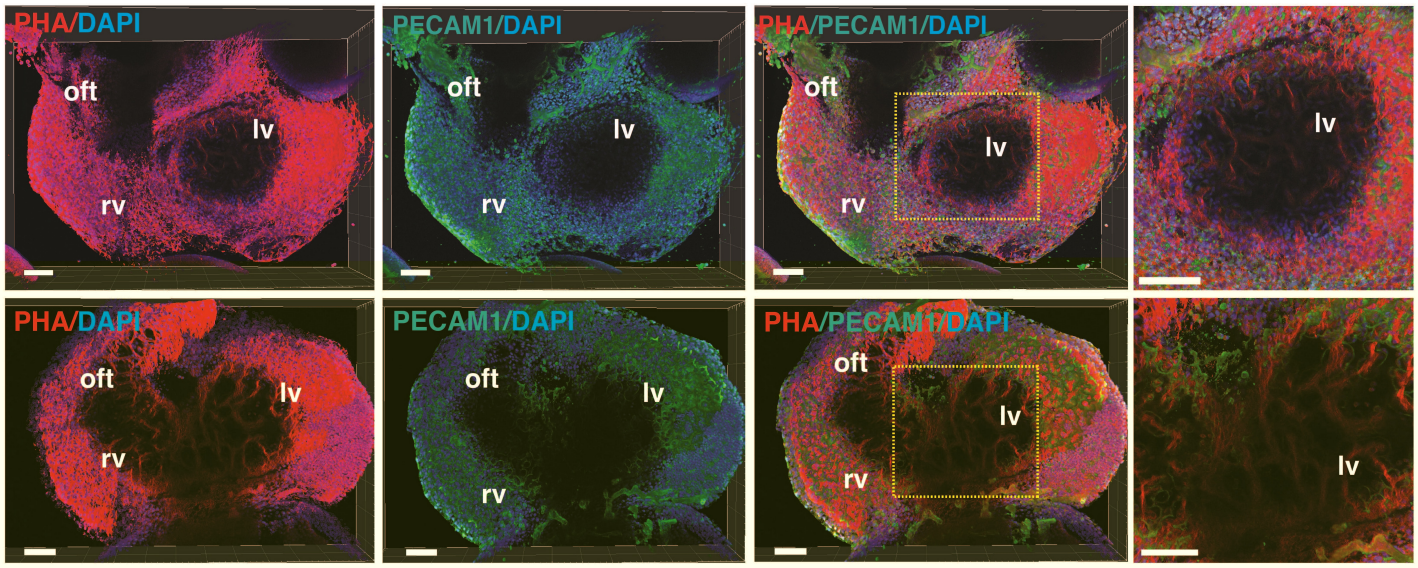

Fig. S8. Usp22 deletion does not cause abnormalities in the organization of developing myocardium and endocardium.
Whole wild-type and Usp22 mutant embryos at E10.0 were stained with phalloidin and anti-PECAM1 antibodies. Two-photon images of embryonic heart chambers were acquired using a Leica multiphoton microscope. rv: right ventricle, lv: left ventricle, oft: outflow tract. Scale bar 100um

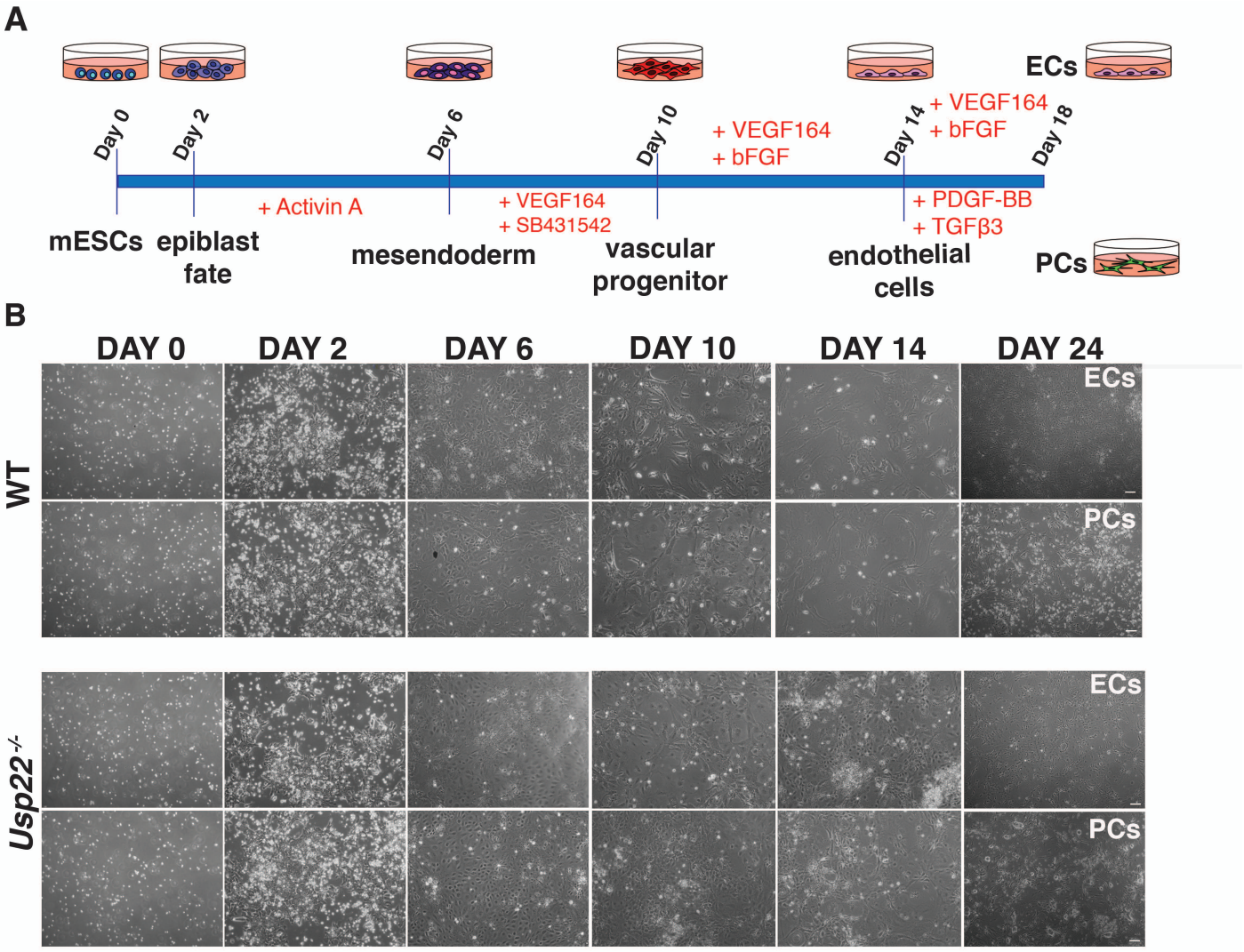

Fig. S9. Differentiation process of mouse embryonic stem cells (mESCs) to endothelial cell lineage or pericyte cell lineage *in vitro*. (A) Timeline of the differentiation protocol followed depicting the growth factors and inhibitors used and the duration of their administration. The protocol is described in detail in the materials and methods. (B) Bright-field images of wild-type and Usp22 $^{-/-}$ mESCs at different stages of their differentiation. Morphological changes upon mesoderm induction (Day 6) and vascular specification (Day 10) are observed in both wild-type and mutant cells. In these time points Usp22 $^{-/-}$ cells show differences in morphology compared to wild-type cells. At day 14 there are also more progenitors in the mutant cells that differentiate to endothelial cells compared to mutant cells at day 24 of the same lineage. Progenitor cells remain present in the Usp22 mutant pericytes' culture at both day 14 and day 24. Scale bar 100um

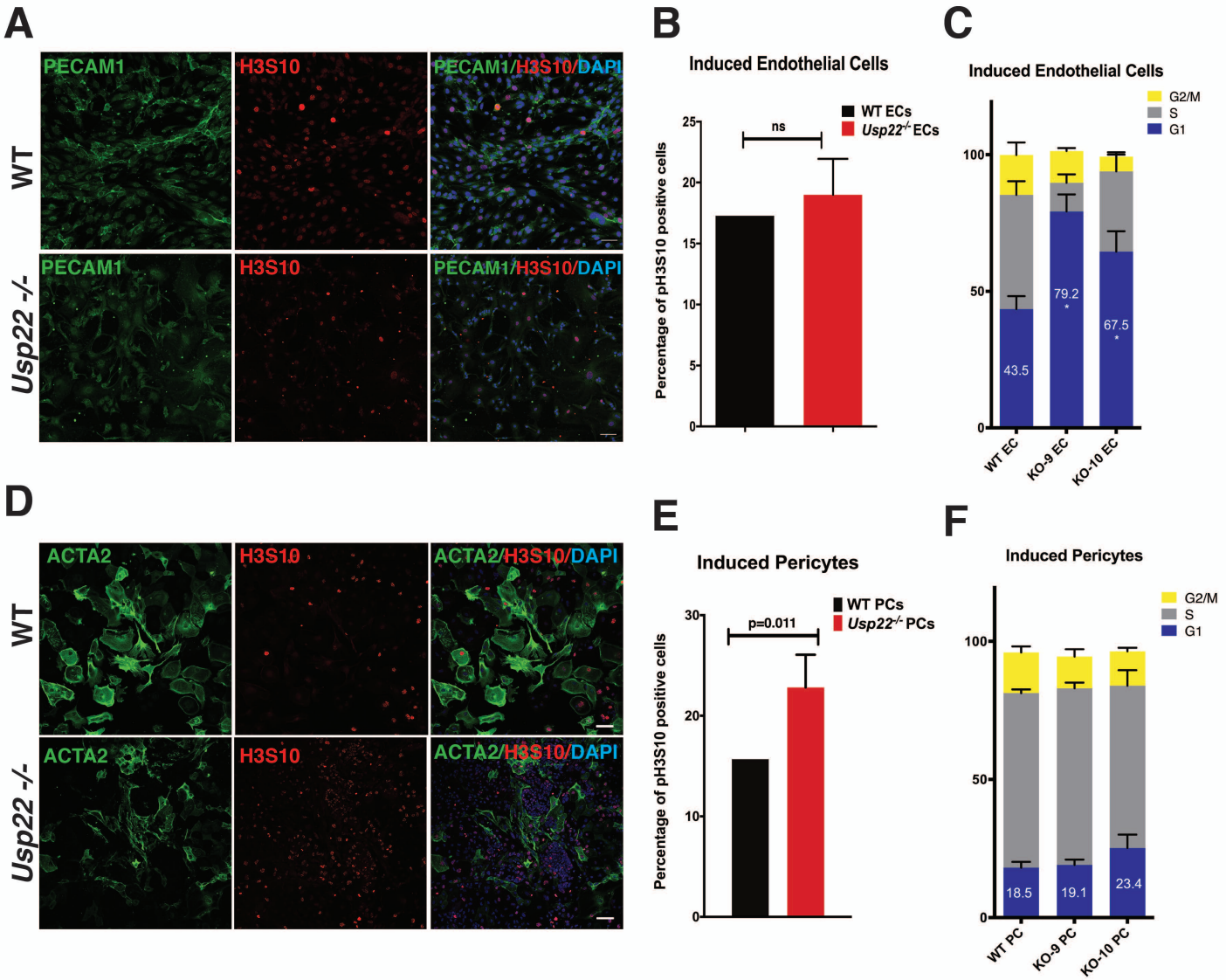

Fig. S10. Usp22 loss of function affects cell proliferation and cell adhesion in induced endothelialcells, but affects cell differentiation and maturation in induced pericytes. (A, D) Confocal imaging of PECAM1 and ACTA2 as markers of induced endothelial cells and pericytes respectively, and mitotic marker H3S10 that shows differences in the proliferation potential of wild-type and Usp22-/- cells. (B, E) Percentage of wild-type and mutant induced endothelial cells and pericytes nuclei positive for phH3S10. Error bars represent SD of at least n=100 nuclei counted in three fields per genotype. (C, F) Analysis of DNA content by flow cytometry shows an increase of G1-phase in the Usp22-/- induced endothelial cells, but not in induced pericytes. Error bar represent SD three technical replicates analyzed per genotype indicated. *p<=0.05 calculated by unpaired t-test with Welch's correction. Scale bar 100um

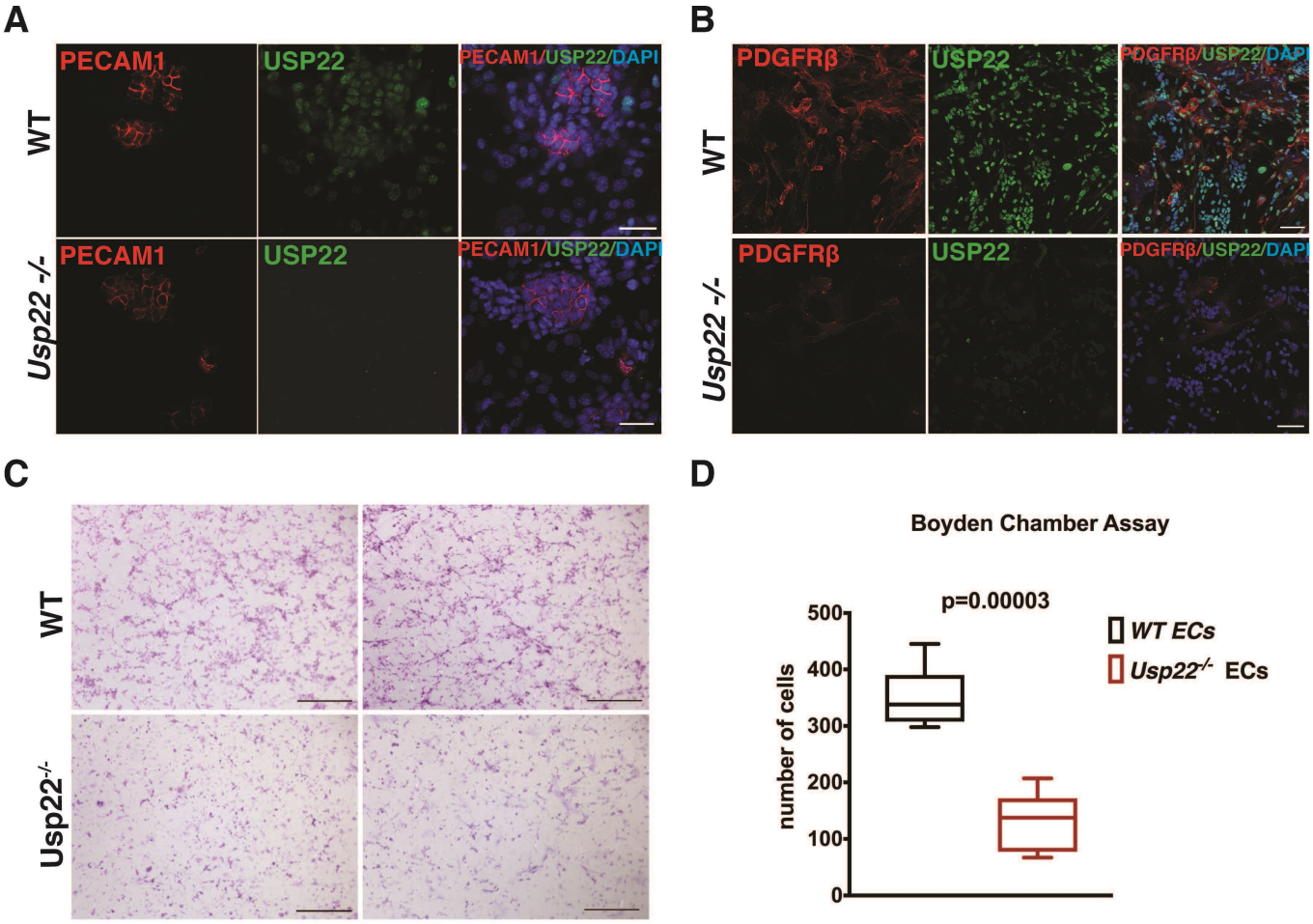

Fig. S11. USP22 localizes in the nuclei of induced endothelial cell progenitors and pericytes and *Usp22* loss of function impairs the migration capacity of induced endothelial cells. (A,B) Confocal imaging of PECAM1 and PDGFRβ as markers of induced endothelial cells and pericytes respectively (passage 0), and USP22 that shows nuclear localization in wild-type cells. Scale bar 100um (C) Representative bright-field images of wild-type and *Usp22* $^{-/-}$ induced endothelial cells stained with crystal violet (passage 4). Scale bar 200um (D) Quantification of migrating induced endothelial cells of the two different genotypes. Error bars represent SD of at least n=100 stained cells counted in three fields per genotype. p<=0.05 calculated by unpaired t-test with Welch's correction.

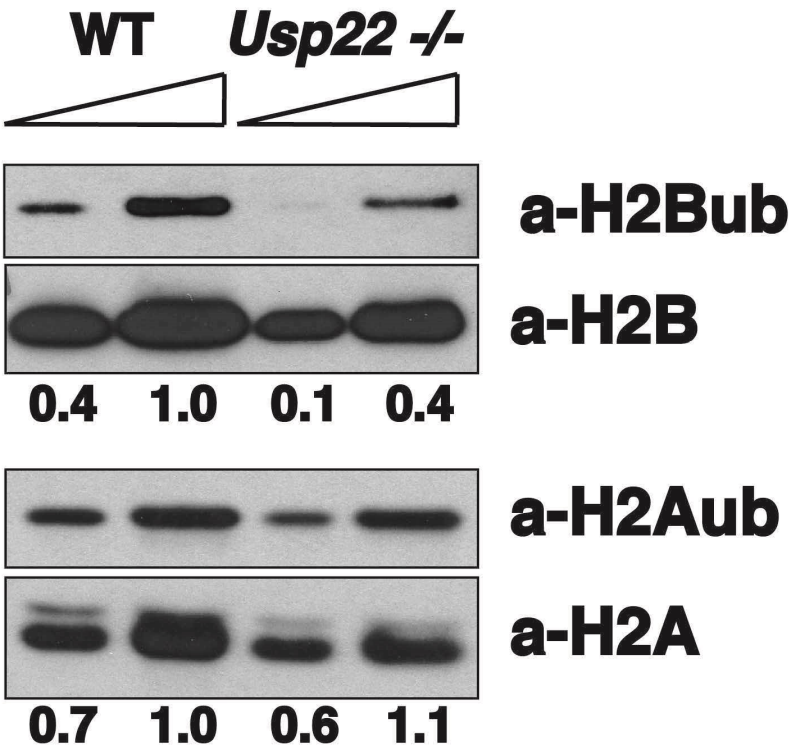

Fig. S12. *Usp22* loss of function in induced endothelial cells does not lead to increased H2B ubiquitination levels. Representative immunoblots showing decreased levels of H2B ubiquitination upon *Usp22* loss of function in induced endothelial cells. The levels of H2A ubiquitination are unaffected by *Usp22* deletion. Quantification of levels of H2A and H2B ubiquitination relative to respective H2A and H2B loading controls was done with ImageJ.

Table S1. Downstream targets of TGFb1 signaling pathway predicted to be inhibited by IPA, that were used for the generation of the heatmap presented in Figure 4F.

Click here to Download Table S1

Table S2. Downstream targets of Erbb2 signaling pathway predicted to be inhibited by IPA, that were used for the generation of the heatmap presented in Figure. 4H.

Click here to Download Table S2

Table S3. Downstream targets of EGF signaling pathway predicted to be inhibited by IPA, that were used for the generation of the heatmap presented in Figure. 4H.

Click here to Download Table S3

Table S4. Downstream targets of HGF signaling pathway predicted to be inhibited by IPA, that were used for the generation of the heatmap presented in Figure. 4H.

Click here to Download Table S4

Table S5. Downstream targets of PDGF signaling pathway predicted to be inhibited by IPA, that were used for the generation of the heatmap presented in Figure. 4H.

Click here to Download Table S5

Table S6. List of antibodies used in the study

Antibody	Source	Cat No	dilution
PROLIFERIN	Santa Cruz	sc-47347	1:500
TPBPA	Abcam	ab104401	1:3000
KI67	Bethyl Lab	IHC-00375-1	1:250
LMNA	Cell Signaling	2035	1:100
PECAM1	Pharmigen	Clone MEC 13.3	1:400
MCT4	EMD Millipore	AB3316P	1:250
ACTA2	Abcam	ab5694	1:250
HIF-1A	Novus Biologicals	NB100-131	1:1000
VEGFA	Santa Cruz	sc-507	1:100
VIMENTIN	Abcam	ab92547	1:500
VCAM1	R&D Systems	AF643	1:200
βCATENIN	BD Biosciences	610153	1:500
VEGFR2 (WB)	Cell Signaling	9698	1:1000
VEGFR2 (IF)	BD Biosciences	555307	1:500
ACTA2	SIGMA	A5228	1:5000
H3S10ph	EMD Millipore	06-570	1:2000
PECAM1	BD Biosciences	550274	1:500
NG2	EMD Millipore	Ab5320	1:500
PDGFRβ	abcam	Ab91066	1:500
USP22	abcam	Ab195289	1:200
Phospho-ERK1/2 (Thr202/Tyr204)	Cell Signaling	4370	1:2000
ERK1/2	Cell Signaling	4695	1:4000
Phospho- AKT (Ser473)	Cell Signaling	4060	1:2000
AKT	Cell Signaling	4691	1:4000
Phospho- COFILIN (Ser3)	Cell Signaling	3311	1:1000
COFILIN	Cell Signaling	5175	1:2000
Phospho-p38MAPK(Thr180/Tyr182)	Cell Signaling	4511	1:1000
p38MAPK	Cell Signaling	9212	1:2000
GAB1	Cell Signaling	3232	1:1000
GAB2	Cell Signaling	3239	1:1000
GRB2	EMD Millipore	05-372	1:1000
PKCα	Cell Signaling	2056	1:1000
PLCγ1	Cell Signaling	5690	1:1000
PDPK1	BD Biosciences	611070	1:1000
SMAD2/3	BD Biosciences	610842	1:1000
HGFR (25H2)	Cell Signaling	3127	1:500
H2Bub	EMD Millipore	05-1312	1:1000
H2B	EMD Millipore	07-371	1:4000
GAPDH	EMD Millipore	mab 374	1:5000
β - TUBULIN	SIGMA	T4026	1:4000

Table S7. List of genomic primers used in the study

Oligo name	Sequence
RRS377-R1for	5'-GGTGGAACCCACGATGGGAG-3'
RRS377-R2rev	5'-GCTGCGGTTGTCAATCACCTCC-3'
RRS377-R3rev	5'-GTGAGGCCAAGTTTGTTTCCTTGAAGGACTCC-3'
RRS377-R5rev	5'-GACCACAGAGAAAGGCTCCTGTCTC-3'
RRS377-bgalrev	5'-AGTATCGGCCTCAGGAAGATCG-3'
XP0208-X1for	5'-GTATTTGCCTGATGTATGTCTGTGTACCAC -3'
XP0208-X2rev	5'-CTCATTCTTATGGCAGCAATGGCAATAAC-3'
XP0208-X3rev	5'-CTTGAGACCTTCTTTCTGGTCTTTCTCTG-3'
XP0208-X5rev	5'-ACTGCCAAATACACCAAGTACCTCCC -3'
XP0208-bgalrev	5'-AGTATCGGCCTCAGGAAGATCG-3'
ZFNUsp22-CellFORSigma	5'-GCTGTAGCCTGCCTGAGTTC-3'
ZFNUsp22-CellREVSigma	5'-CCTCTCCCTCTCCCACCTAC-3'
RRS377 - 5'probeFOR	5'-GCCTCAAACTCAGCAATCCTCC-3'
RRS377 - 5'probeREV	5'-CAGGGCCATGACTCCAACACAC-3'
RRS377 - 3'probeFOR	5'-CCAGATGATGATGGTGATGGC-3'
RRS377 - 3'probeREV	5'-GACGGCAGGGAACAGATGTAG-3'
XP0208 - 5'probeFOR	5'-GCCTCAAACTCAGCAATCCTCC-3'
XP0208 - 5'probeREV	5'-CAGGGCCATGACTCCAACACAC-3'
XP0208 - 3'probeFOR	5'-CCAGATGATGATGGTGATGGC-3
XP0208 - 3'probeREV	5'-GACGGCAGGGAACAGATGTAG-3'

Table S8. List of qRT-PCR primers used in the study

Oligo Name	Sequence
mProliferinF	TGAGCCCAGACACGTTAGAA
mProliferinR	GAATTAGCCGGCAGTTTGTC
mPrl3d1F	GGGAGAATGTGTCCTCCAAA
mPrl3d1R	ATCTGCGGCCAAGATAAATG
mTpbpAF	CTCTTGCAGTTCAGCATCCA
mTpbpAR	GCACAGCTTTGGACATCACA
mPrdm1F	TAGACTTCACCGATGAGGGG
mPrdm1R	GTATGCTGCCAACAACAGCA
mMct4F	TCGTCTCTCTCCACAAATGG
mMct4R	CTAGGGAAGACAGCTGCCAC
mCebpaF	GCAGTGTGCACGTCTATGCT
mCebpaR	AAGTCTTAGCCGGAGGAAGC
mPECAM1F	AGTTGCTGCCCATTCATCAC
mPECAM1R	CTGGTGCTCTATGCAAGCCT
mCtsqF	CCAAACTGGGATCAAATGCT
mCtsqR	GAGGCAGTAGTGGTCATCCC
mCcna2F	TGATAGATGCTGACCCGTACCTT
mCcna2R	CTCTGGTGGGTTGAGAAGAGAAA
mCcne1F	TTGAATTGGGGCAATAGAGAAGA
mCcne1R	AGTCCTGTGCCAAGTAGAACGTC
mCcne2F	GTGCATTCTAGCCATCGACTCTT
mCcne2R	AGGCACCATCCAGTCTACACATT
mCdkn1cF	TTCTCCTGCGCAGTTCTCTT
mCdkn1cR	CTGAAGGACCAGCCTCTCTC
mPumaF	CACCTAGTTGGGCTCCATTT
mPumaR	ACCTCAACGCGCAGTACG
mCdkn1aF	ATCACCAGGATTGGACATGG
mCdkn1aR	CGGTGTCAGAGTCTAGGGGA
mBcl2F	AGGGTCTTCAGAGACAGCCA
mBcl2R	AGTACCTGAACCGGCATCTG
mFlt4F	CCCTGCAGGATATGGATAGG
mFlt4R	GCTCTGCCTCGGACTCCT
mHif-2AF	ATCACGGGATTTCTCCTTCC
mHif-2AR	GGTTAAGGAACCCAGGTGCT
mHif-3AF	CCAGCAACTTCTGCAATCCT
mHif-3AR	GCAATGCCTGGTGCTTATCT
mAdmF	AACCAGCTTCATTCTGTGGC

mAdmR	TGGACTTTGGGGTTTTGCTA
mHif-1AF	AAACTTCAGACTCTTTGCTTCG
mHif-1AR	CGGCGAGAACGAGAAGAA
mHif-1BF	CAGCTCCTCCACCTTGAATC
mHif-1BR	GGCGACTACAGCTAACCCAG
mCited2F	CATATGGTCTGCCATTTCCA
mCited2R	ATCGGCTGTCCCTCTATGTG
mTgfb1F	AAGTTGGCATGGTAGCCCTT
mTgfb1R	GCCCTGGATACCAACTATTGC
mTgfbr1F	GCAAAGACCATCTGTCTCACA
mTgfbr1R	CTCCTCATCGTGTTGGTGG
mBcl6F	AGAACATCACTAGCGTGCCG
mBcl6R	AGTTTCTAGGAAAGGCCGGA
mSmad2F	TTTGCTGTACTCAGTCCCCA
mSmad2R	TGAGCTTGAGAAAGCCATCA
mSmad3F	ACAGGCGGCAGTAGATAACG
mSmad3R	AACGTGAACACCAAGTGCAT
mGab1F	TCTTGGCATGATCGTTTTTG
mGab1R	CGGAGAAGAAGTTGAAGCGT
mGab2F	GGGTTTCTTGGAGTGCTCAT
mGab2R	CCTCCCGAGAAGAAGTTGAG
mGrb2F	GTCATATTTGGCGATGGCTT
mGrb2R	GTGCAAGAATAGCCCCAGAA
mAkt1F	GCCGTTCCTTGTAGCCAATA
mAkt1R	CATGAACGACGTAGCCATTG
mPdpk1F	CACCACACTGGACTGAATGG
mPdpk1R	GGATGAGGACGCTGAGGAG
mGcm1F	CTCCTGGAACCAGTCAGTCG
mGcm1R	AGCCTGTGTTGAGCAGACCT
mCD9F	TCCAATAGCAAGCACTGCAA
mCD9R	CGGTCAAAGGAGGTAGCAAG
mHgfrF	TGTCCGATACTCGTCACTGC
mHgfrR	CATTTTTACGGACCCAACCA
mHgfF	CTTCTCCTTGGCCTTGAATG
mHgfR	CCTGACACCACTTGGGAGTA
mMct1F	ATCGCAGGTGGCATTTTAAG
mMct1R	GTCACGCATACTCCGGGC
mSynAF	GATGACATCCACTGCCACAC
mSynAR	ATTGTCCGGCTCGAATAGG
mSynBF	GACCGTTTCTTCGAATCTGC
mSynBR	CAAGGTCTCAGCATATGCCA
mDlx3F	CGGTTCTGGAACCAGATTTT
mDlx3R	CGTTTCCAGAAAGCCCAGTA
mOvol2F	CTCTTGCCACAAAGGTCACA

mOvol2R	ATGGACATCTGGCAGCGAT
mNr6a1F	GTTCAGCTCGATCATCTGGG
mNr6a1R	TGTCAGGATGAATTGGCAGA
mCrb3F	CCTTTCACAAATAGCACAACTCAAC
mCrb3R	AGAAACAGTCCCACTGCTATAAGG
mPdgfBF	GAAGATCATCAAAGGAGCGG
mPdgfBR	CCTTCCTCTCTGCTGCTACC
mPdgfrbF	TGGCCTCTGAGGACTAAAGC
mPdgfrbR	AACAGAAGACAGCGAGGTGG
mActa2F	GTTCAGTGGTGCCTCTGTCA
mActa2R	ACTGGGACGACATGGAAAAG
mCdh5F	CGTTGGACTTGATCTTTCCC
mCdh5R	CGCCAAAAGAGAGACTGGAT
mMmp9F	GTGGTTCAGTTGTGGTGGTG
mMmp9R	CCCGCTGTATAGCTACCTCG
mPlauF	GAAGGTGCAAACGTCCACTT
mPlauR	GGACCCAGAGTGGAAAACAG
mLama3F	ACAGCAAGTCAGTCCAGCTC
mLama3R	CCGATCACCACACTGTCGAT
mCfl1F	GCCTTCTTGCGTTTCTTCAC
mCfl1R	TCTGTCTCCCTTTCGTTTCC
mp38MAPKF	TCTTAACTGCCACACGATGC
mp38MAPKR	GAACAAGACCATCTGGGAGG
mHand1F	CTTTAATCCTCTTCTCGCCG
mHand1R	TGAACTCAAAAAGACGGATGG
mPrl2c5F	AGCCCAGGCACGTTAGAATA
mPrl2c5R	ACATTTGAATTAGCCGGCAG
mMash2F	TCCATCAAGCTTGCATTCAG
mMash2R	GAAGGTGCAAACGTCCACTT